Dynamics of a three-level atom in a two-mode squeezed vacuum

W. K. Lai, V. Bužek,* and P. L. Knight

Optics Section, Blackett Laboratory, Imperial College, London SW7 2BZ, England

(Received 1 April 1991)

In this paper we study the dynamics of a three-level atom interacting with a two-mode squeezed vacuum, a highly correlated state in which each mode contains the same number of quanta yet exhibits a thermal photon distribution. Under exact resonance, the Rabi oscillations exhibit an irregular behavior reminiscent of those in the thermal-state Jaynes-Cummings model. If the individual field modes are sufficiently detuned from the intermediate atomic level, the Rabi oscillations become quasiperiodic. The three-level system in this case reduces to an effective two-level system in which two-photon processes dominate. The times of revivals of the Rabi oscillations in this limit depend only on the atom-field coupling constants and the detuning. For comparison, we present a parallel study of the case in which the initial field is prepared in an uncorrelated two-mode state, such as a two-mode thermal state or a two-mode coherent state. Under the full resonance condition, the former leads to an irregular evolution of the Rabi oscillations, while the latter leads to the usual collapse and revival phenomena. If the individual modes are sufficiently detuned from the intermediate atomic level, we observe the same quasiperiodicity of the Rabi oscillations as in the case of the two-mode squeezed vacuum but with a doubling of revival times (for equal atom-field coupling constants). Whereas the two-mode squeezed vacuum and the two-mode thermal-state transition dynamics lead to correlation between the field modes, the two-mode coherent state leads to anticorrelation (when sufficiently detuned from the intermediate atomic level).

I. INTRODUCTION

A subject of considerable interest in quantum optics concerns the interaction of atoms with quantized fields [1]. The prototype of such problems is the ordinary Jaynes-Cummings model (JCM) [2], in which a two-level atom interacts with a single mode of the electromagnetic radiation field. This model is exactly solvable in the rotating-wave approximation and yields purely quantum features in the system dynamics, such as the collapse and revival of the Rabi oscillations [3], the squeezing of the electromagnetic field [4], and sub-Poissonian photo-counting statistics [5]. Recent experiments with Rydberg atoms in high-Q microwave cavities have led to the observation of some of these effects [6].

Various extensions of the ordinary JCM have been made. These include multiphoton generalizations of the JCM [7]; the addition of a further atomic level to support a second resonance [8]; and cooperative effects in multiatom systems [9]. In this paper we shall concentrate on the second category of problems. Namely, we shall take a three-level atom in the λ configuration and two quantized modes of the electromagnetic field. In a previous paper [10] we treated such a problem in which the field is prepared in the SU(2) coherent state [11], where the modes are *anticorrelated*. It was shown that the anticorrelation between the modes can lead to purely periodic behavior of the Rabi oscillations. Our motivation in the present study is to investigate the effect of intermode field *correlations* (in particular those associated with the two-mode squeezed vacuum [12]) on the system dynamics.

The two-mode squeezed vacuum is a highly nonclassi-cal state of the electromagnetic field in which each mode contains the same number of quanta and each exhibits a thermal photon distribution, whereas a superposition of the modes shows a reduction in noise below the quantum limit [13]. The interaction of this state of light with a three-level atom is particularly interesting. Under the full resonance condition, the Rabi oscillations are shown here to exhibit an irregular behavior reminiscent of those in the ordinary JCM with the initial field prepared in the thermal state [14]. Moreover, we find that on allowing the individual modes to be sufficiently detuned from the intermediate level (see Fig. 1), the Rabi oscillations revive *periodically* and *independently* of the intensity of the initial field. In fact the revival times depend only on the atom-field coupling constants and the detuning. The initial correlation of the field in this case is shown to reduce the revival times of the Rabi oscillations. Moreover, because we have started from an exact three-level system, the induced Stark shifts from the dominant levels are implicitly included [15], and are shown to play an important role in the atomic dynamics, both for correlated and uncorrelated fields.

We should point out that studies of the interactions of three-level atoms with uncorrelated fields have been carried out previously [8,16–18]. In particular, Li and Peng [18] considered a three-level atom in the λ configuration interacting with a quantized field prepared either in the two-mode coherent state or the two-mode thermal state. They examined the atomic populations for these fields under the full resonant and off-one-photon resonance conditions, and showed that the effect of coherent and chaotic sources are different even at low intensities. They failed, however, to note the periodicity of the revival
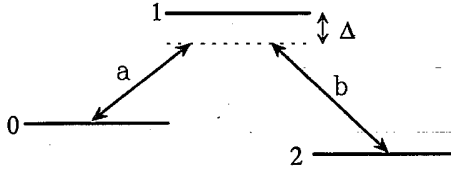
FIG. 1. Energy-level diagram for a three-level atom in the λ configuration interacting with two quantized modes of the electromagnetic radiation field, with a one-photon detuning Δ.

times and their independence from the intensity of the initial field in the far-off-one-photon resonance limit.

Recently, Gerry and Eberly [19] studied the interaction of a Raman coupled model [20] with two quantized modes of the electromagnetic field. The Raman coupled model is a special case of the three-level atom in which the excited state is considered to be far-off resonance [8] and is adiabatically eliminated [15]. It is described by an effective Hamiltonian containing products of the transition operators between two lower state levels and a field annihilation operator from one mode and a creation operator from the other. Moreover, the induced Stark shifts can be included by assuming that the resulting two-level system is no longer two-photon resonant, but is detuned by an intensity-dependent amount. However, it is this latter aspect of the problem that Gerry and Eberly neglected in their study, and as we will show, this leads to quite different evolutions. In fact the Stark shifts play an important role in the system dynamics even for low-intensity fields. Indeed there is evidence that they observably distort one-atom maser line shapes by amounts which are determined by the field photon statistics [21].

Another aspect of the present paper concerns the evolution of the field statistics, in particular the field correlation between modes. In the two-mode squeezed vacuum, the modes are initially correlated, with the degree of correlation being governed by the number of excitations in each mode [13]. In the presence of the atom-field interaction it is shown that under the full resonance condition, all three field states studied here, the two-mode squeezed vacuum, the two-mode thermal state, and the two-mode coherent state, lead to an average increase in correlation between the modes. But when the detuning from the intermediate level is sufficiently large, we find that while the modes of the two-mode squeezed vacuum

and the two-mode thermal state remain correlated, those of the two-mode coherent state become anticorrelated.

We organize this paper as follows. In Sec. II we introduce our model of the three-level atom interacting with two quantized field modes, followed in Sec. III by a consideration of the far-off-one-photon resonance limit. Then in Secs. IV–VII we present a numerical study of the atomic and field dynamics, concluding in Sec. VIII with a summary of our results.

II. MODEL

Our three-level atomic system shown in Fig. 1 consists of two allowed transitions, $0\leftrightarrow1$ and $1\leftrightarrow2$, each interacting with a different mode of the field. We assume for simplicity the two-photon resonance condition, but otherwise we allow the individual modes to be detuned by an arbitrary amount Δ from the intermediate atomic level. With these assumptions, the interaction Hamiltonian in the rotating wave approximation is given by

$$H_I = \hbar\Delta R_{11} + \hbar[g_a(a^\dagger R_{01} + R_{10}a) + g_b(b^\dagger R_{21} + R_{12}b)] ,$$

(2.1)

where $R_{ij} \equiv |i\rangle\langle j|$ are the atomic operators; a,b and $a^\dagger,b^\dagger$ are the annihilation and creation operators of the respective field modes; and g_a and g_b are the atom-field coupling constants.

We suppose that the initial state vector of the field may be written in the form

$$|\Psi(0)\rangle_f = \sum_{n_a,n_b} \tilde{Q}_{n_a,n_b}|n_a,n_b\rangle ,$$

(2.2)

where $|n_a,n_b\rangle \equiv |n_a\rangle\otimes|n_b\rangle$. The associated joint photon distribution is related to the expansion coefficients $\tilde{Q}_{n_a,n_b}$ by

$$\tilde{P}_f(n_a,n_b) = |\tilde{Q}_{n_a,n_b}|^2 .$$

(2.3)

Similarly, we suppose that the atom starts in the ground-state level $|0\rangle$, so that the state vector of the total atom-field system may be written in the factored form

$$|\Psi(0)\rangle = |0\rangle\otimes|\Psi(0)\rangle_f .$$

(2.4)

At time t the atom and field states are coupled by the interaction and evolve according to

$$|\Psi(t)\rangle = \sum_{n_a,n_b} \tilde{Q}_{n_a,n_b}[C_0(n_a,n_b,t)|0;n_a,n_b\rangle + C_1(n_a,n_b,t)|1;n_a-1,n_b\rangle + C_2(n_a,n_b,t)|2;n_a-1,n_b+1\rangle] ,$$

(2.5)

where the coefficients $C_i(n_a,n_b,t)$ are determined from the time-dependent Schrödinger equation, and are given as follows:

$$C_0(n_a,n_b,t) = \frac{\Omega_{n_b}^2}{\Omega_{n_a-1,n_b}^2} + \frac{\Omega_{n_a}^2-1}{\Omega_{n_a-1,n_b}^2}\left[\cos\tilde{\Omega}_{n_a-1,n_b}t + i\frac{\delta}{\tilde{\Omega}_{n_a-1,n_b}}\sin\tilde{\Omega}_{n_a-1,n_b}t\right]e^{-i\delta t} ,$$

$$C_1(n_a,n_b,t) = -i\frac{\Omega_{n_a}-1}{\tilde{\Omega}_{n_a-1,n_b}}e^{-i\delta t}\sin\tilde{\Omega}_{n_a-1,n_b}t ,$$

(2.6)

$$C_2(n_a,n_b,t) = -\frac{\Omega_{n_a-1}\Omega_{n_b}}{\Omega^2_{n_a-1,n_b}}\left[1-\left[\cos\widetilde{\Omega}_{n_a-1,n_b}t + i\frac{\delta}{\widetilde{\Omega}_{n_a-1,n_b}}\sin\widetilde{\Omega}_{n_a-1,n_b}t\right]e^{-i\delta t}\right].$$

Here the various Rabi frequencies are defined by

$$\Omega_{n_{a(b)}} = g_{a(b)}\sqrt{n_{a(b)}+1}\;,$$

$$\Omega_{n_a-1,n_b} = \sqrt{\Omega^2_{n_a-1}+\Omega^2_{n_b}}\;, \qquad (2.7)$$

$$\widetilde{\Omega}_{n_a-1,n_b} = \sqrt{\Omega^2_{n_a-1,n_b}+\delta^2}\;,$$

with $\delta = \Delta/2$. The atomic occupation probabilities in the (n_a,n_b)th manifold are obtained using

$$P_i(n_a,n_b,t) = |C_i(n_a,n_b,t)|^2\;, \quad i=0,1,2 \qquad (2.8)$$

and are given as follows:

$$P_0(n_a,n_b,t) = \frac{\Omega^4_{n_b}}{\Omega^4_{n_a-1,n_b}} + \frac{\Omega^4_{n_a-1}}{\Omega^4_{n_a-1,n_b}}\left[\cos^2\widetilde{\Omega}_{n_a-1,n_b}t + \frac{\delta^2}{\widetilde{\Omega}^2_{n_a-1,n_b}}\sin^2\widetilde{\Omega}_{n_a-1,n_b}t\right]$$

$$+ \frac{2\Omega^2_{n_a-1}\Omega^2_{n_b}}{\Omega^4_{n_a-1,n_b}}\left[\cos\widetilde{\Omega}_{n_a-1,n_b}t\,\cos\delta t + \frac{\delta}{\widetilde{\Omega}_{n_a-1,n_b}}\sin\widetilde{\Omega}_{n_a-1,n_b}t\,\sin\delta t\right],$$

$$P_1(n_a,n_b,t) = \frac{\Omega^2_{n_a-1}}{\widetilde{\Omega}^2_{n_a-1,n_b}}\sin^2\widetilde{\Omega}_{n_a-1,n_b}t\;, \qquad (2.9)$$

$$P_2(n_a,n_b,t) = \frac{\Omega^2_{n_a-1}\Omega^2_{n_b}}{\widetilde{\Omega}^4_{n_a-1,n_b}}\left[1 + \cos^2\widetilde{\Omega}_{n_a-1,n_b}t + \frac{\delta^2}{\widetilde{\Omega}^2_{n_a-1,n_b}}\sin^2\widetilde{\Omega}_{n_a-1,n_b}t\right.$$

$$\left. -2\left[\cos\widetilde{\Omega}_{n_a-1,n_b}t\,\cos\delta t + \frac{\delta}{\widetilde{\Omega}_{n_a-1,n_b}}\sin\widetilde{\Omega}_{n_a-1,n_b}t\,\sin\delta t\right]\right].$$

In the following section we will consider the large one-photon detuning limit of Eq. (2.9).

III. THE FAR-OFF-ONE-PHOTON RESONANCE LIMIT

The dynamics of the three-level system becomes particularly simple when we take the large one-photon detuning limit. To show this, we define a small parameter ϵ by

$$\epsilon_{n_a-1,n_b} = \frac{\Omega_{n_a-1,n_b}}{\Delta} \ll 1 \qquad (3.1)$$

and expand the amplitudes of the system of equations (2.8) to order unity in ϵ. The result is given by

$$P_0(n_a,n_b,t) \approx 1 - \frac{4\Omega^2_{n_a-1}\Omega^2_{n_b}}{\Omega^4_{n_a-1,n_b}}\sin^2\frac{\Omega^2_{n_a-1,n_b}t}{2\Delta}\;,$$

$$P_1(n_a,n_b,t) \approx 0\;, \qquad (3.2)$$

$$P_2(n_a,n_b,t) \approx \frac{4\Omega^2_{n_a-1}\Omega^2_{n_b}}{\Omega^4_{n_a-1,n_b}}\sin^2\frac{\Omega^2_{n_a-1,n_b}t}{2\Delta}\;.$$

From Eq. (3.2) it follows that in the large-detuning limit, the probability of occupation of the intermediate atomic level is vanishingly small and may be adiabatically eliminated, reducing the three-level system to an effective two-level system [15]. This is seen more concretely if we

define an effective coupling constant κ and an intensity-dependent detuning $\widetilde{\Delta}_{n_a,n_b}$ by

$$\kappa = \frac{g_a g_b}{\Delta}\;,$$

$$\widetilde{\Delta}_{n_a-1,n_b} = \frac{\Omega^2_{n_a-1}-\Omega^2_{n_b}}{\Delta}(1-\delta_{n_a 0}\delta_{n_b 0})\;. \qquad (3.3)$$

We can then recast Eq. (3.2) in the form

$$P_+(n_a,n_b,t) = 1 - \frac{\kappa^2_{n_a-1,n_b}}{\widetilde{\kappa}^2_{n_a-1,n_b}}\sin^2\widetilde{\kappa}_{n_a-1,n_b}t\;,$$

$$\qquad (3.4)$$

$$P_-(n_a,n_b,t) = \frac{\kappa^2_{n_a-1,n_b}}{\widetilde{\kappa}^2_{n_a-1,n_b}}\sin^2\widetilde{\kappa}_{n_a-1,n_b}t\;,$$

which are readily recognized as the solutions for a two-state system with levels $+$ and $-$ (see Fig. 2). The quantities κ_{n_a-1,n_b} and $\widetilde{\kappa}_{n_a-1,n_b}$ are the effective and generalized Rabi frequencies defined by

$$\kappa_{n_a-1,n_b} = \frac{\Omega_{n_a-1}\Omega_{n_b}}{\Delta} = \kappa\sqrt{n_a(n_b+1)}\;,$$

$$\widetilde{\kappa}_{n_a-1,n_b} = \sqrt{\kappa^2_{n_a-1,n_b}+\tfrac{1}{4}\widetilde{\Delta}^2_{n_a-1,n_b}}\;. \qquad (3.5)$$
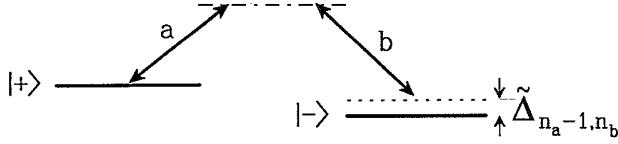
FIG. 2. The Raman coupled model with two quantized modes a and b, driving transitions via a virtual state from state $|+\rangle$ to a $|-\rangle$, both of which are Stark shifted.

Of course, in this limit we could have started from an effective two-level Hamiltonian with Stark shifted transition frequencies and a two-photon coupling,

$$H = \hbar\omega_a a^\dagger a + \hbar\omega_b b^\dagger b + \hbar\hat{\omega}_+ R_{++} + \hbar\hat{\omega}_- R_{--}$$
$$+ \frac{\hbar g_a g_b}{\Delta}(a^\dagger b R_{+-} + R_{-+} b^\dagger a) , \qquad (3.6)$$

where $R_{+-} \equiv |+\rangle\langle -|$, and $\hat{\omega}_+$ and $\hat{\omega}_-$ are the intensity-dependent transition frequencies defined by

$$\hat{\omega}_+ = \omega_0 + \frac{g_a^2}{\Delta} a^\dagger a ,$$
$$\hat{\omega}_- = \omega_2 + \frac{g_b^2}{\Delta} b^\dagger b . \qquad (3.7)$$

The last terms in Eq. (3.7) are due to ac Stark shifts of levels 1 and 2, respectively.

Finally, we would like to point out from Eqs. (3.2) or (3.4) that the proper inclusion of the Stark shifts has resulted in a *linear* dependence of the Rabi frequency $\tilde{\kappa}_{n_a-1,n_b}$ on the photon numbers n_a and n_b. Had we neglected the Stark shifts, we would have arrived at the solutions

$$P_+(n_a,n_b,t) = \cos^2\kappa_{n_a-1,n_b}t ,$$
$$P_-(n_a,n_b,t) = \sin^2\kappa_{n_a-1,n_b}t , \qquad (3.8)$$

as if the two-photon-resonant levels were driven by an effective coupling constant of 2κ as shown by Gerry and Eberly [19], rather than the correct value of κ. Further, it is seen that the Rabi frequency in Eq. (3.8) depends on the square root of the product of n_a and $n_b + 1$, rather than a linear dependence on them required for large detunings as in Eq. (3.2) for a two-photon process. It is therefore vital that Stark shifts are included in any analysis of multiphoton effective two-level systems.

IV. ATOMIC DYNAMICS

In this section we present a numerical study of the dynamics of a three-level atom interacting with correlated and uncorrelated states of the electromagnetic field. The quantities of interest are the atomic occupation probabilities defined by

$$P_i(t) = \sum_{n_a,n_b} \tilde{P}_f(n_a,n_b) P_i(n_a,n_b,t) , \quad i = 0,1,2 \qquad (4.1)$$

where $\tilde{P}_f(n_a,n_b)$ is the joint photon distribution of the in-

itial field and $P_i(n_a,n_b,t)$ are the atomic occupation probabilities in the (n_a,n_b)th manifold. Section IV A will deal with a field prepared in the two-mode squeezed vacuum, while Secs. IV B and IV C will deal with fields prepared in the two-mode thermal state and the two-mode coherent state, respectively.

A. Two-mode squeezed vacuum

The two-mode squeezed vacuum has been widely studied in connection with nonclassical states of the electromagnetic field [12–13], and has recently been realized in the laboratory [22]. In its number-state representation, it takes the form [13]

$$|\xi\rangle = \frac{1}{\cosh r} \sum_{n=0}^{\infty} e^{in\theta} \tanh r |n,n\rangle , \qquad (4.2)$$

where the squeezing parameter $\xi = re^{i\theta}$. The correlation between the modes of the two-mode squeezed vacuum is immediately apparent in Eq. (4.2), where it is seen that each mode contains the same number of quanta. Barnett and Phoenix [23], using their index of correlation, have shown that the two-mode squeezed vacuum is the most correlated of all two-mode states of light.

The joint photon distribution for the two-mode squeezed vacuum is obtained straightforwardly from Eq. (4.2) and is given by

$$\tilde{P}_f(n_a,n_b) = \frac{\bar{n}^{n_a}}{(1+\bar{n})^{n_a+1}} \delta_{n_a n_b} , \qquad (4.3)$$

where $\bar{n} = \sinh^2 r$ is the mean number of photons in each mode. The marginal photon distributions are obtained by tracing over the appropriate mode variable and are given by

$$\tilde{P}_f^a(n) = \tilde{P}_f^b(n) = \tilde{P}_f(n) = \frac{\bar{n}^n}{(1+\bar{n})^{n+1}} . \qquad (4.4)$$

It follows therefore that the photon statistics of the individual modes of the two-mode squeezed vacuum are thermal in character [13].

For the two-mode squeezed vacuum, the double summation in Eq. (4.1) for the atomic occupation probabilities reduces to a single summation due to the tight photon correlation (the delta function δ_{n_a,n_b}) between the modes,

$$P_i(t) = \sum_{n=0}^{\infty} \tilde{P}_f(n) P_i(n,n,t) , \quad i = 0,1,2 . \qquad (4.5)$$

In Fig. 3 we display the results of Eq. (4.5) for various values of the one-photon detuning Δ. The value of $\bar{n}$ chosen corresponds to about 95% squeezing in the normal mode quadrature operators. At zero detuning, the Rabi oscillations are irregular, rather like those of the ordinary JCM with the initial field prepared in the thermal state [14]. This observation is readily intelligible because at zero detuning, one photon processes play a significant role in the system dynamics, and therefore, as the individual modes of the two-mode squeezed vacuum are
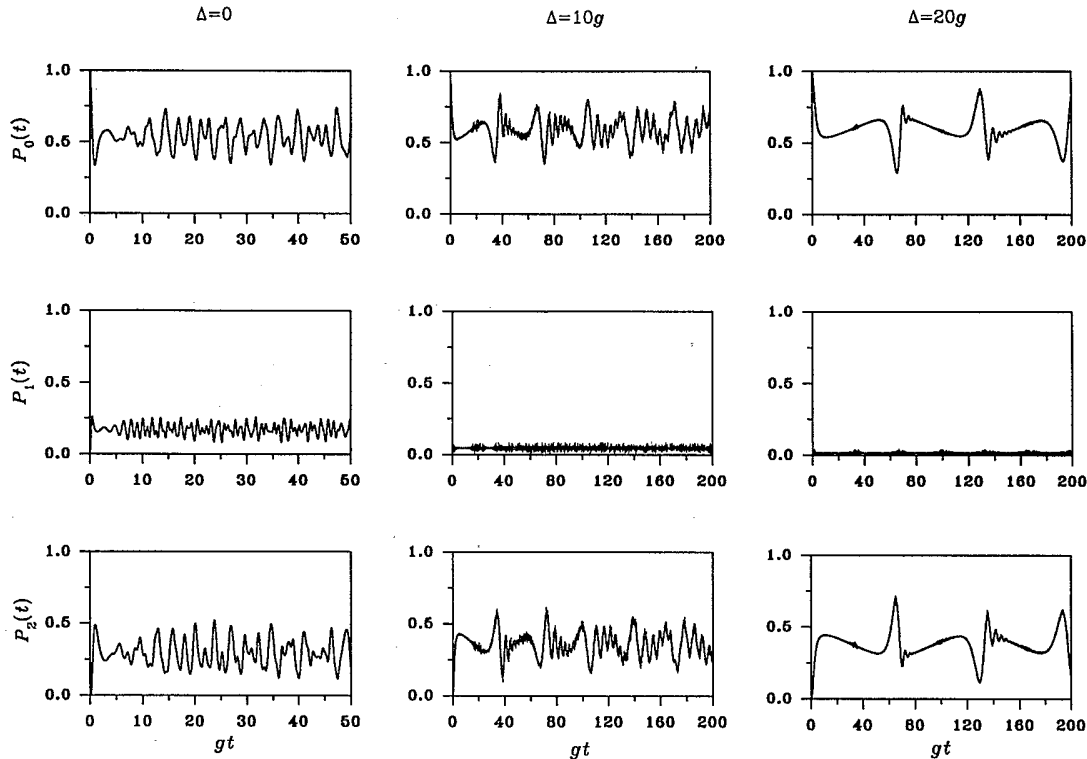
FIG. 3. Time evolution of the atomic occupation probabilities when the initial field is prepared in the two-mode squeezed vacuum with the number of excitations in each mode $\bar{n}$ equal to 4. The atom-field coupling constants are equal, $g_a = g_b = g$.

thermal in character, the atomic occupation probabilities should reflect this feature. However, on increasing the detuning, we observe a transition from irregular behavior to an apparently quasiperiodic behavior. The three-level system in this limit is an effective two-level system in which two-photon processes dominate. The Rabi oscillations revive periodically and independently of the intensity of the initial field. Its origin may be traced back to the

linear dependence of the effective Rabi frequency on the photon numbers (in the large one-photon detuning limit) so that the photon statistical averages become sums of *commensurate* Rabi oscillations.

To estimate the revival times of the Rabi oscillations in the limit of large one-photon detuning, we follow an analogous procedure given in Refs. [8,19]. First, we write the probability of occupation of level 0 in the form

$$
P_0(t) = \sum_{n=0}^{\infty} \widetilde{P}_f(n) \left[\frac{\Omega_{n_a-1}^4 + \Omega_{n_b}^4}{\Omega_{n_a-1,n_b}^4} + \frac{2\Omega_{n_a-1}^2\Omega_{n_b}^2}{\Omega_{n_a-1,n_b}^4} \cos\frac{\Omega_{n_a-1,n_b}^2 t}{\Delta} \right]
$$

$$
= \mathrm{Re}\left\{ \sum_{n=0}^{\infty} \widetilde{P}_f(n) \left[\frac{\Omega_{n_a-1}^4 + \Omega_{n_b}^4}{\Omega_{n_a-1,n_b}^4} + \frac{2\Omega_{n_a-1}^2\Omega_{n_b}^2}{\Omega_{n_a-1,n_b}^4} \exp\left[\frac{i\Omega_{n_a-1,n_b}^2 t}{\Delta} \right] \right] \right\}, \tag{4.6}
$$

and then we assume that the dominant contribution in the summation comes from the term for which $n \approx n_0$, where n_0 is the photon number for which $\widetilde{P}_f(n)$ is maximum. To single out this dominant term we rewrite Ω_{n_a-1,n_b}^2 as

$$
\Omega_{n_a-1,n_b}^2 = \Omega_{n_0-1,n_0}^2 + (g_a^2 + g_b^2)(n - n_0) \tag{4.7}
$$

and then substitute Eq. (4.7) back into Eq. (4.6), giving

$$
P_0(t) = \mathrm{Re}\left\{ \exp\left[\frac{i\Omega_{n_0-1,n_0}^2 t}{\Delta} \right] \sum_{n=0}^{\infty} \widetilde{P}_f(n) \left[\frac{\Omega_{n_a-1}^4 + \Omega_{n_b}^4}{\Omega_{n_a-1,n_b}^4} \exp\left[\frac{-i\Omega_{n_0-1,n_0}^2 t}{\Delta} \right] + \frac{2\Omega_{n_a-1}^2\Omega_{n_b}^2}{\Omega_{n_a-1,n_b}^4} \exp\left[\frac{i(g_a^2 + g_b^2)(n - n_0)t}{\Delta} \right] \right] \right\}.
$$

$$
\tag{4.8}
$$

The times of revivals t_r of the Rabi oscillations occur whenever the phase in the last exponential of Eq. (4.8) is a multiple of 2π, i.e.,

$$\frac{(g_a^2+g_b^2)t_r}{\Delta}=2\pi k \ , \quad k=1,2,\dots \tag{4.9}$$

or

$$t_r=\frac{2\pi k\Delta}{g_a^2+g_b^2} \ . \tag{4.10}$$

Thus in the large-one-photon-detuning limit, the revival times are independent of the intensity of the initial field. The result (4.10) is in good agreement with the numerical plots of Fig. 3 from the solution of the full equations of motion. It should be noted that for the sake of brevity, we have used the term revival to mean a reinitiation of the time-dependent evolution of the atomic populations after a period of quiescent collapse. Strictly speaking, only the times t_r in Eq. (4.10) for which k is an even number correspond to true revivals of the Rabi oscillations, as seen when we substitute $t=t_r$ into Eq. (4.6), giving

$$P_0(t=t_r^{(k)})=\sum_{n=0}^{\infty}\widetilde{P}_f(n)\left\{\frac{\Omega_{n_a-1}^4+\Omega_{n_b}^4}{\Omega_{n_a-1,n_b}^4}+\frac{2\Omega_{n_a-1}^2\Omega_{n_b}^2}{\Omega_{n_a-1,n_b}^4}\cos\left[\left(n+\frac{g_b^2}{g_a^2+g_b^2}\right)2\pi k\right]\right\} \ . \tag{4.11}$$

From Eq. (4.11) it readily follows that when the atom-field coupling constants are equal, only even values of k will give rise to constructive interference among the various terms comprising the sum (and hence a revival of the Rabi oscillations); odd values of k will give rise to destructive interference, leading to a minimum in $P_0(t)$.

B. Two-mode thermal state

The two-mode thermal state is characterized by the density matrix [24]

$$\widetilde{\rho}=\widetilde{\rho}_a\otimes\widetilde{\rho}_b \ , \tag{4.12}$$

where $\widetilde{\rho}_a$ and $\widetilde{\rho}_b$ are given by

$$\widetilde{\rho}_i=\sum_{n_i=0}^{\infty}\frac{\bar{n}_i^{n_i}}{(1+\bar{n}_i)^{n_i+1}}|n_i\rangle\langle n_i| \ , \quad i=a,b \ . \tag{4.13}$$

From Eqs. (4.12) and (4.13) it follows that the joint and marginal photon distributions for the two-mode thermal state are given by
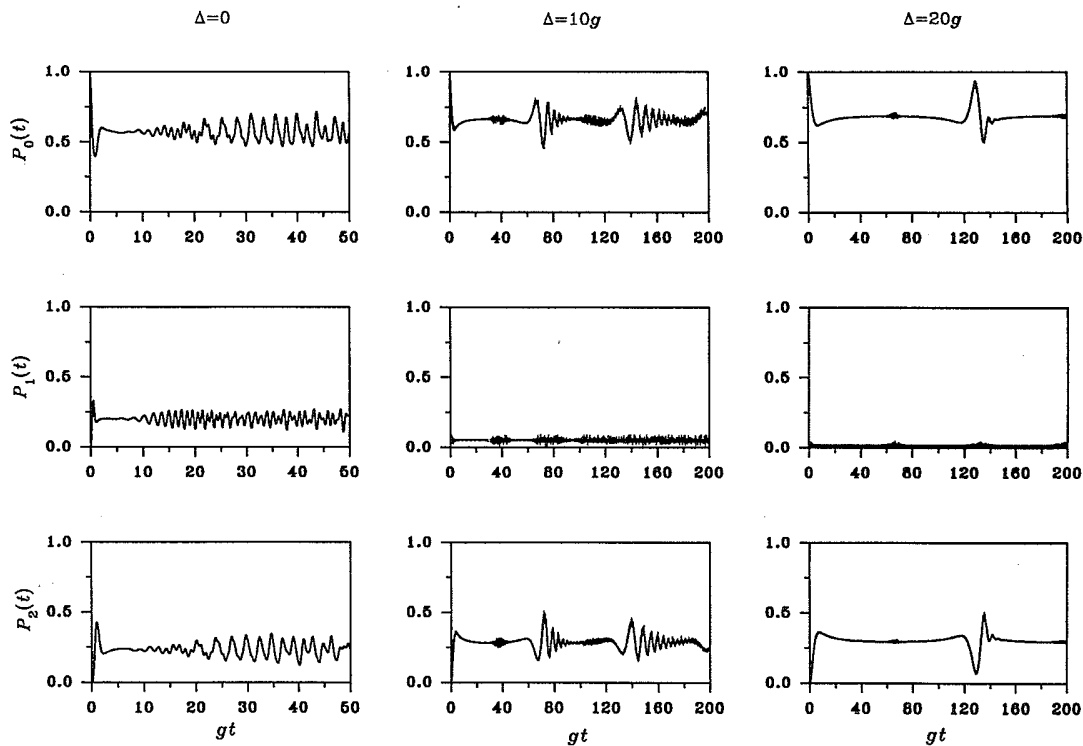

FIG. 4. Same as in Fig. 3 but with the field in the two-mode thermal state.

$$\tilde{P}_f(n_a, n_b) = \tilde{P}_f^a(n_a)\tilde{P}_f^b(n_b) ,$$

$$\tilde{P}_f^a(n_a) = \frac{\bar{n}_a^{n_a}}{(1+\bar{n}_a)^{n_a+1}} , \quad\quad (4.14)$$

$$\tilde{P}_f^b(n_b) = \frac{\bar{n}_b^{n_b}}{(1+\bar{n}_b)^{n_b+1}} .$$

In what follows we have chosen the distributions such that the photon statistics for the individual modes of the two-mode thermal state are the same as those for the two-mode squeezed vacuum.

In Fig. 4 we plot the atomic occupation probabilities for a field initially prepared in the two-mode thermal state (4.12). A general feature of the graphs which immediately comes to mind is that the amplitudes of the Rabi oscillations are somewhat smaller than those of the corresponding ones for the two-mode squeezed vacuum. We can understand this by realizing that when the modes are uncorrelated the total effective field is *smaller* than

when the modes are correlated. The other feature which we see is a transition from irregular evolution to an apparently quasiperiodic evolution when the one-photon detuning is made sufficiently large. As with the two-mode squeezed vacuum, we can trace this back to the linear dependence of the effective Rabi frequency $\tilde{\kappa}_{n_a-1,n_b}$ in Eq. (3.4) on the photon numbers. Closer examination of the revival times for the two-mode thermal state reveals that they are twice those of the corresponding revival times for the two-mode squeezed vacuum (for the particular values of atom-field coupling constants chosen) in the limit of large one-photon detuning. Thus one way of distinguishing between correlated and uncorrelated fields of the *same* marginal photon statistics is through the difference in the revival times of the Rabi oscillations in the large-one-photon-detuning limit.

To estimate the revival time of the Rabi oscillations in the large-one-photon-detuning limit, we again adopt an analogous procedure given in Refs. [8,19]. That is, we rewrite the probability of occupation of level 0 in the form

$$P_0(t) = \text{Re}\left\{ \exp\left[\frac{i\Omega_{n_{0a}-1,n_{0b}}^2 t}{\Delta}\right] \sum_{n_a=0}^{\infty}\sum_{n_b=0}^{\infty} \tilde{P}_f(n_a, n_b) \left[\frac{\Omega_{n_a-1}^4 + \Omega_{n_b}^4}{\Omega_{n_a-1,n_b}^4}\exp\left[\frac{-i\Omega_{n_{0a}-1,n_{0b}}^2 t}{\Delta}\right] \right.\right.$$

$$\left.\left. + \frac{2\Omega_{n_a-1}^2\Omega_{n_b}^2}{\Omega_{n_a-1,n_b}^4}\exp\left[\frac{ig_a^2(n_a-n_{0a})t}{\Delta}\right]\exp\left[\frac{ig_b^2(n_b-n_{0b})t}{\Delta}\right] \right] \right\} ,$$

$$(4.15)$$

where we have divided Ω_{n_a-1,n_b}^2 into two parts,

$$\Omega_{n_a-1,n_b}^2 = \Omega_{n_{0a}-1,n_{0b}}^2 + g_a^2(n_a-n_{0a}) + g_b^2(n_b-n_{0b}) . \quad (4.16)$$

Here n_{0a} and n_{0b} are the photon numbers for which the joint photon distribution $\tilde{P}_f(n_a, n_b)$ is maximum. The Rabi oscillations revive whenever

$$\frac{g_a^2 t_r}{\Delta} = 2\pi k , \quad k=1,2,\ldots$$

$$\frac{g_b^2 t_r}{\Delta} = 2\pi l , \quad l=1,2,\ldots . \quad (4.17)$$

Multiplying and dividing these two expressions, we obtain the conditions for the revival times t_r as follows:

$$t_r = \frac{2\pi\sqrt{m}\,\Delta}{g_a g_b} , \quad m=kl=1,2,\ldots$$

$$\frac{g_a^2}{g_b^2} = \frac{k}{l} . \quad (4.18)$$

Comparing Eqs. (4.18) and (4.10) it is readily seen that uncorrelated fields lead to longer revival times for the

Rabi oscillations. The result (4.18) applies for *any* uncorrelated two-mode states of the field in the large-one-photon-detuning limit.

C. Two-mode coherent state

The two-mode coherent state is defined by [24]

$$|\alpha_a, \alpha_b\rangle = \exp[-\tfrac{1}{2}(|\alpha_a|^2+|\alpha_b|^2)]$$

$$\times \sum_{n_a=0}^{\infty}\sum_{n_b=0}^{\infty} \frac{\alpha_a^{n_a}}{\sqrt{n_a!}}\frac{\alpha_b^{n_b}}{\sqrt{n_b!}}|n_a, n_b\rangle , \quad (4.19)$$

with joint and marginal photon distributions given by

$$\tilde{P}_f(n_a, n_b) = \tilde{P}_f^a(n_a)\tilde{P}_f^b(n_b) ,$$

$$\tilde{P}_f^a(n_a) = \frac{\bar{n}_a^{n_a}}{n_a!}\exp(-\bar{n}_a) , \quad\quad (4.20)$$

$$\tilde{P}_f^b(n_b) = \frac{\bar{n}_b^{n_b}}{n_b!}\exp(-\bar{n}_b) ,$$

where $\bar{n}_a$ and $\bar{n}_b$ are the mean photon numbers in modes a and b, respectively.

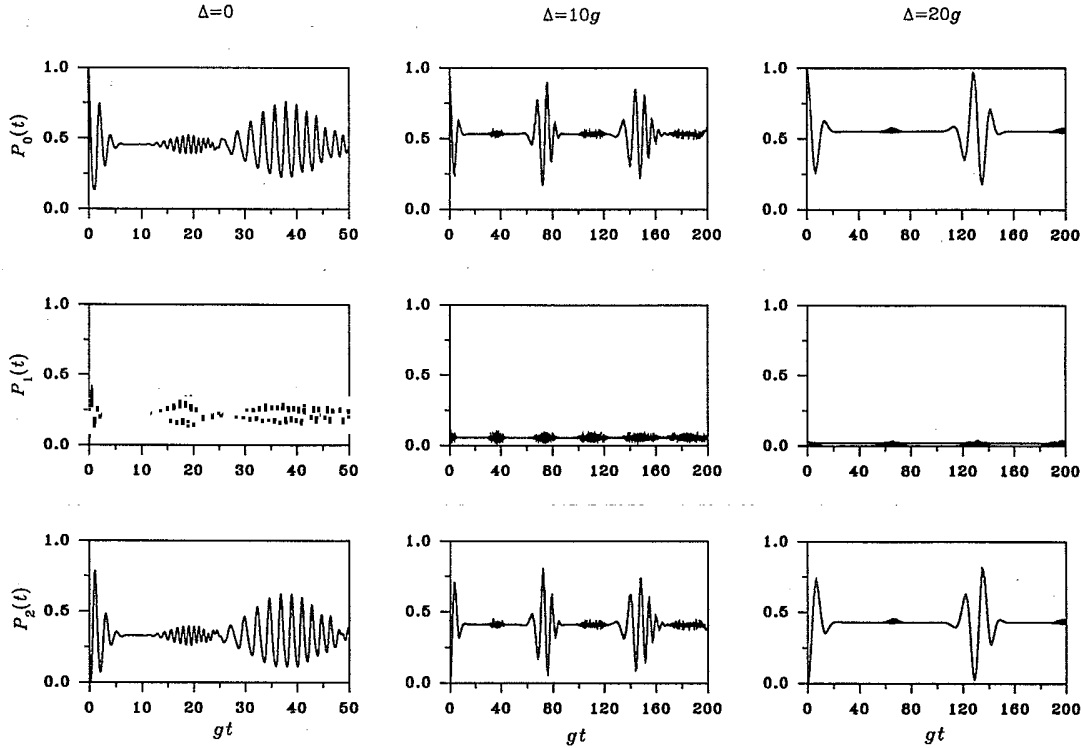In Fig. 5 we plot the atomic occupation probabilities

FIG. 5. Same as in Fig. 3 but with the field in the two-mode coherent state.

for a field initially prepared in the two-mode coherent state. At zero one-photon detuning we see the usual collapse and revival of Rabi oscillations. We note further that there two types of Rabi oscillations, one at a smaller amplitude than the other. These are attributed to one- and two-photon processes, respectively. As we increase the one-photon detuning, we see a gradual decrease in the amplitudes of the one-photon Rabi oscillations, and a gradual increase in the periodicity of the revivals of the two-photon Rabi oscillations. The revival times estimated using Eq. (4.18) are found to be in good agreement with the numerical plots of Fig. 5.

V. TIME-AVERAGED ATOMIC DYNAMICS

In this section we investigate the mean behavior of the three-level atom through the time-averaged occupation probabilities [25]

$$\bar{P}_i = \lim_{T \to \infty} \frac{1}{T} \int_0^T dt\, P_i(t) , \quad i = 0,1,2 . \tag{5.1}$$

Using Eq. (4.1) we find

$$\bar{P}_i = \sum_{n_a, n_b} \tilde{P}_f(n_a, n_b) \bar{P}_i(n_a, n_b) , \tag{5.2}$$

where

$$\bar{P}_i(n_a, n_b) = \lim_{T \to \infty} \frac{1}{T} \int_0^T dt\, P_i(n_a, n_b, t) , \tag{5.3}$$

from which we obtain

$$\bar{P}_0(n_a, n_b) = \frac{\Omega_{n_b}^4}{\Omega_{n_a-1,n_b}^4} + \frac{\Omega_{n_a-1}^4}{2\Omega_{n_a-1,n_b}^4} \left[1 + \frac{\delta^2}{\tilde{\Omega}_{n_a-1,n_b}^2} \right] ,$$

$$\bar{P}_1(n_a, n_b) = \frac{\Omega_{n_a-1}^2}{2\tilde{\Omega}_{n_a-1,n_b}^2} , \tag{5.4}$$

$$\bar{P}_2(n_a, n_b) = \frac{\Omega_{n_a-1}^2 \Omega_{n_b}^2}{\Omega_{n_a-1,n_b}^4} + \frac{\Omega_{n_a-1}^2 \Omega_{n_b}^2}{2\Omega_{n_a-1,n_b}^4} \left[1 + \frac{\delta^2}{\tilde{\Omega}_{n_a-1,n_b}^2} \right] .$$

In the limit of large one-photon detuning the expressions (5.4) reduce to the simpler forms

$$\bar{P}_0(n_a, n_b) \approx 1 - \frac{1}{2} \frac{\kappa_{n_a-1,n_b}^2}{\tilde{\kappa}_{n_a-1,n_b}^2} ,$$

$$\bar{P}_1(n_a, n_b) \approx 0 , \tag{5.5}$$

$$\bar{P}_2(n_a, n_b) \approx \frac{1}{2} \frac{\kappa_{n_a-1,n_b}^2}{\tilde{\kappa}_{n_a-1,n_b}^2} ,$$

where κ_{n_a-1,n_b} and $\tilde{\kappa}_{n_a-1,n_b}$ are defined as before.

In Fig. 6 we plot the time-averaged atomic occupation probability $\bar{P}_0$ as a function of the mean photon number in each mode of the field. We have chosen a detuning such that the two-level approximation to the three-level system remains valid for the range of mean photon numbers considered. What clearly emerges from the plot in
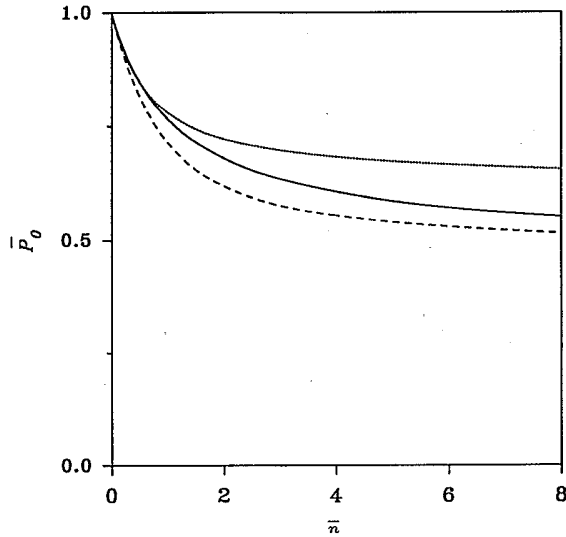
FIG. 6. Time-averaged occupation probability of level 0 as a function of the mean photon number in each mode. The solid, dotted and dashed lines are for fields prepared in the two-mode squeezed vacuum, the two-mode thermal state, and the two-mode coherent state, respectively. The one-photon detuning Δ was set to 20g.
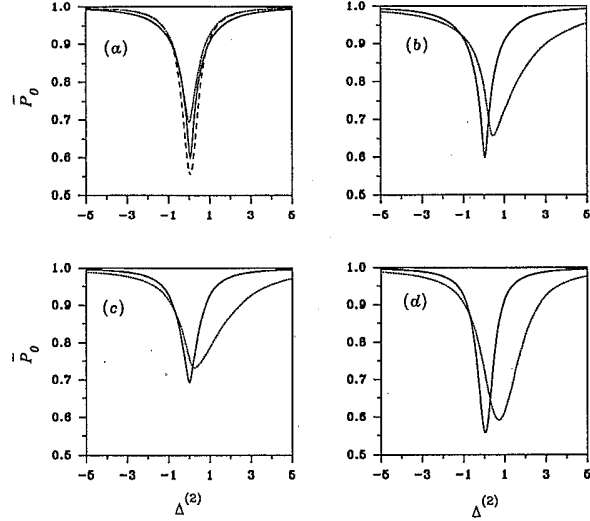
FIG. 7. Time-averaged occupation probability of level 0 as function of the intensity-independent two-photon detuning $\Delta^{(2)}$. The solid, dotted, and dashed lines in (a) are for fields prepared in the two-mode squeezed vacuum, the two-mode thermal state, and the two-mode coherent state, respectively. The atom-field coupling constants are equal. (b)–(d) display the results for the three fields separately. The solid and dotted lines are for equal $(g_a = g_b = g = 1)$ and nonequal $(g_a = 1, g_b = 2)$ atom-field coupling constants, respectively. In all cases the one-photon detuning was set to 20g.

Fig. 6 is that $\bar{P}_0$ is higher if the initial field is prepared in the two-mode thermal state, rather than the two-mode squeezed vacuum or the two-mode coherent state. At first glance, it seems rather puzzling that $\bar{P}_0$ should be different at all for the two-mode squeezed vacuum and the two-mode thermal state, given they each have the same marginal photon statistics. The answer to this puzzle lies in the fact that the spread in the induced intensity-dependent detuning $\tilde{\Delta}$ is far greater if the field is prepared in the two-mode thermal state rather than the two-mode squeezed vacuum and reflects the correlations between the modes rather than the mean photon numbers which determine the mean shift. We will discuss this point in more detail later.

In experiments a quantity which is often measured is the probability of the atom staying in its initial state as the frequency of the exciting field is swept, or equivalently as the system is detuned from exact resonance. In what follows we shall assume that the two-level approximation to the three-level system is valid, that is, we assume a large one-photon detuning. Then the results (5.5) are easily generalized to include an intensity-independent two-photon detuning $\Delta^{(2)}$:

$$\bar{P}_0(n_a, n_b) \approx 1 - \frac{1}{2} \frac{\kappa_{n_a-1,n_b}^2}{\tilde{\kappa}_{n_a-1,n_b}^{\prime 2}} ,$$

$$\bar{P}_1(n_a, n_b) \approx 0 , \qquad (5.6)$$

$$\bar{P}_2(n_a, n_b) \approx \frac{1}{2} \frac{\kappa_{n_a-1,n_b}^2}{\tilde{\kappa}_{n_a-1,n_b}^{\prime 2}} ,$$

where $\tilde{\kappa}_{n_a-1,n_b}^{\prime}$ is defined as

$$\tilde{\kappa}_{n_a-1,n_b}^{\prime} = \sqrt{\kappa_{n_a-1,n_b}^2 + \tfrac{1}{4}(\Delta^{(2)} - \tilde{\Delta}_{n_a-1,n_b})^2} . \qquad (5.7)$$

We should stress that the system of equations (5.6) are valid only in the limit $\Delta^{(2)} \ll \Delta$ and that condition (3.1) is satisfied.

In Fig. 7(a) we plot $\bar{P}_0$ as a function of the intensity-independent two-photon detuning for three initial states of the field. We have chosen the atom-field coupling constants such that $g_a = g_b = g$. A first observation shows that the transition line shapes are symmetric for all three initial states of the field and that they are shifted by the same small amounts. When the atom-field coupling constants are such that $g_a \neq g_b$, the transition line shapes become asymmetric as well as being broader and are shifted by greater amounts, as shown in Figs. 7(b)–7(d) for the two-mode squeezed vacuum, the two-mode thermal state, and the two-mode coherent state, respectively. As we shall see, these features can be attributed to the induced Stark shifts of levels 0 and 2.

We showed in Sec. III that in the limit of large one-photon detuning, the three-level atomic system reduces to an effective two-level system. Further, we showed that the atomic occupation probabilities in the (n_a, n_b)th manifold are simply given by

$$P_0(n_a, n_b, t) \approx 1 - \frac{\kappa^2_{n_a-1,n_b}}{\tilde{\kappa}^2_{n_a-1,n_b}} \sin^2 \tilde{\kappa}_{n_a-1,n_b} t ,$$

$$P_1(n_a, n_b, t) \approx 0 , \qquad\qquad (5.8)$$

$$P_2(n_a, n_b, t) \approx \frac{\kappa^2_{n_a-1,n_b}}{\tilde{\kappa}^2_{n_a-1,n_b}} \sin^2 \tilde{\kappa}_{n_a-1,n_b} t ,$$

where the generalized two-photon Rabi frequency $\tilde{\kappa}_{n_a-1,n_b}$ is defined by

$$\tilde{\kappa}_{n_a-1,n_b} = \sqrt{\kappa^2_{n_a-1,n_b} + \tfrac{1}{4}\tilde{\Delta}^2_{n_a,n_b}} \qquad (5.9)$$

and $\tilde{\Delta}_{n_a-1,n_b}$ is the induced intensity-dependent detuning defined by

$$\tilde{\Delta}_{n_a-1,n_b} = \frac{\Omega^2_{n_a-1} - \Omega^2_{n_b}}{\Delta}(1 - \delta_{n_a 0}\delta_{n_b 0}) . \qquad (5.10)$$

Using Eq. (5.10) we can calculate the mean and variance of the induced detuning for the three initial states of the field. The results are easily obtained, and are given by

$$E^c(\tilde{\Delta}) = \frac{g_a^2 - g_b^2}{\Delta}\langle n \rangle - \frac{g_b^2}{\Delta}[1 - \tilde{P}_f(0)] ,$$

$$\qquad\qquad\qquad\qquad\qquad (5.11)$$

$$V^c(\tilde{\Delta}) = \frac{(g_a^2 - g_b^2)^2}{\Delta^2}\langle \Delta n^2 \rangle$$

$$+ \frac{g_b^2}{\Delta^2}\{g_b^2[1 - \tilde{P}_f(0)] - 2(g_a^2 - g_b^2)\langle n \rangle\}\tilde{P}_f(0) ,$$

for the two-mode squeezed vacuum, and

$$E^{uc}(\tilde{\Delta}) = \frac{g_a^2\langle n_a \rangle - g_b^2\langle n_b \rangle}{\Delta} - \frac{g_b^2}{\Delta}[1 - \tilde{P}_f(0,0)] ,$$

$$\qquad\qquad\qquad\qquad\qquad (5.12)$$

$$V^{uc}(\tilde{\Delta}) = \frac{g_a^4\langle \Delta n_a^2 \rangle + g_b^4\langle \Delta n_b^2 \rangle}{\Delta^2}$$

$$+ \frac{g_b^2}{\Delta^2}\{g_b^2[1 - \tilde{P}_f(0,0)]$$

$$- 2(g_a^2\langle n_a \rangle - g_b^2\langle n_b \rangle)\}\tilde{P}_f(0,0)$$

for the uncorrelated two-mode thermal and coherent states. When the atom-field coupling constants are equal and the marginal photon statistics (for the uncorrelated two-mode states) are the same, expressions (5.11) and (5.12) reduce to the simpler forms

$$E^c(\tilde{\Delta}) = -\frac{g^2}{\Delta}[1 - \tilde{P}_f(0)] ,$$

$$V^c(\tilde{\Delta}) = \frac{g^4}{\Delta^2}[1 - \tilde{P}_f(0)]\tilde{P}_f(0) ,$$

$$\qquad\qquad\qquad\qquad\qquad (5.13)$$

$$E^{uc}(\tilde{\Delta}) = -\frac{g^2}{\Delta}[1 - \tilde{P}_f(0,0)] ,$$

$$V^{uc}(\tilde{\Delta}) = \frac{2g^4}{\Delta^2}\langle \Delta n^2 \rangle + \frac{g^4}{\Delta^2}[1 - \tilde{P}_f(0,0)]\tilde{P}_f(0,0) .$$

From Eqs. (5.13) it follows that the uncorrelated two-

mode states produce a greater spread in the induced detuning $\tilde{\Delta}$ than the correlated two-mode squeezed vacuum [as seen from the dependence of $V^{uc}(\tilde{\Delta})$ on the photon number spread Δn^2]. The consequence of this is evident in Fig. 6, where the time-averaged occupation probability of the atomic level 0 is greater in the presence of the two-mode thermal states than in the two-mode squeezed vacuum, even though both exhibit the same photon statistics in their individual modes.

A convenient measure of the role of the Stark shifts in the time-averaged atomic dynamics is obtained by calculating the deviation $\bar{P}_i - \bar{P}'_i$, where $\bar{P}'_i$ is the time-averaged occupation probability of level i in the absence of the Stark shifts. From Eqs. (5.2) and (5.8) we find

$$\bar{P}_0 = \sum_{n_a, n_b} \tilde{P}_f(n_a, n_b)\left[1 - \frac{1}{2}\frac{\kappa^2_{n_a-1,n_b}}{\tilde{\kappa}^2_{n_a-1,n_b}}\right] ,$$

$$\bar{P}'_0 = \tfrac{1}{2}[1 + \tilde{P}^a_f(0)] , \qquad\qquad (5.14)$$

giving

$$\bar{P}_0 - \bar{P}'_0 = \frac{1}{2}\left[\sum_{n_a=0}^{\infty}\sum_{n_b=0}^{\infty}\tilde{P}_f(n_a, n_b)\left[\frac{\Omega^2_{n_a-1} - \Omega^2_{n_b}}{\Omega^2_{n_a-1,n_b}}\right]^2\right.$$

$$\left. - \tilde{P}^a_f(0)\right] . \qquad\qquad (5.15)$$

For the two-mode squeezed vacuum, the double summation in Eq. (5.15) reduces to a single summation:

$$\bar{P}_0 - \bar{P}'_0 = \frac{1}{2}\left[\sum_{n=0}^{\infty}\tilde{P}_f(n)\left[\frac{\Omega^2_{n_a-1} - \Omega^2_{n_b}}{\Omega^2_{n_a-1,n_b}}\right]^2 - \tilde{P}_f(0)\right] .$$

$$\qquad\qquad\qquad\qquad\qquad (5.16)$$

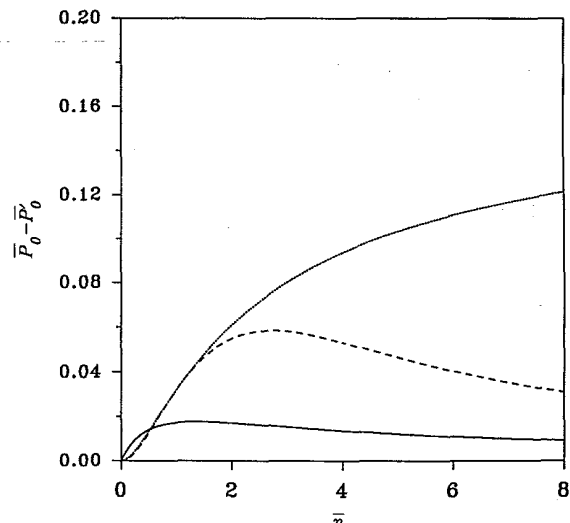In Fig. 8 we plot $\bar{P}_0 - \bar{P}'_0$ as a function of the mean pho-

FIG. 8. A measure of the role of Stark shifts in the large-one-photon-detuned three-level atom as function of the mean photon number in each mode.

ton number in each mode for three initial states of the field. For the particular choice of coupling constants $(g_a = g_b)$, the Stark shifts play a greater role in the time-averaged atomic dynamics if the initial field is prepared in an uncorrelated two-mode state, in particular the two-mode thermal state.

VI. FIELD DYNAMICS

In this section we turn our attention to a study of the field dynamics, in particular the time evolution of the photon distributions and the correlations (or anticorrelations) between the field modes. We start by calculating the joint photon distribution at time t, which from Eq. (2.4), is given by

$$P_f(n_a, n_b, t) = \tilde{P}_f(n_a, n_b) P_0(n_a, n_b, t)$$
$$+ \tilde{P}_f(n_a + 1, n_b) P_1(n_a + 1, n_b, t)$$
$$+ \tilde{P}_f(n_a + 1, n_b - 1)$$
$$\times P_2(n_a + 1, n_b - 1, t) . \qquad (6.1)$$

The marginal photon distributions are obtained by tracing out the appropriate mode variable:

$$P_f^{a(b)}(n_{a(b)}, t) = \sum_{n_{b(a)}} P_f(n_a, n_b, t) . \qquad (6.2)$$

Equations (6.1) and (6.2) apply for both correlated and uncorrelated two-mode states of the field. In particular, for the two-mode squeezed vacuum, we find the following expressions for the time-dependent photon distributions:

$$P_f(n_a, n_b, t) = \tilde{P}_f(n_a) P_0(n_a, n_a, t) \delta_{n_a, n_b} + \tilde{P}_f(n_a + 1) P_1(n_a + 1, n_a + 1, t) \delta_{n_b, n_a + 1} + \tilde{P}_f(n_a + 1) P_2(n_a + 1, n_a + 1, t) \delta_{n_b, n_a + 2} ,$$

$$P_f^a(n, t) = \tilde{P}_f(n) P_0(n, n, t) + \tilde{P}_f(n + 1)[1 - P_0(n + 1, n + 1, t)] , \qquad (6.3)$$

$$P_f^b(n, t) = \tilde{P}_f(n - 1) P_2(n - 1, n - 1, t) + \tilde{P}_f(n)[1 - P_2(n, n, t)] ,$$

from which it follows that the atom-field interaction significantly alters the photon distributions from their initial forms.

The development of correlation or anticorrelation between the field modes is determined by the normalized cross-correlation function [24]

$$g^{(2)}(t) = \frac{\langle n_a n_b \rangle_t}{\langle n_a \rangle_t \langle n_b \rangle_t} , \qquad (6.4)$$

where the subscript means that the expectation values are taken at time t. Written in this form, the cross-correlation function is a measure of the time-dependent coincidence counting of a and b photons. If $g^{(2)}$ is less than unity, we say that the photons of mode a and b are anticorrelated, otherwise they are correlated.

For the two-mode squeezed vacuum, the relevant quantities in the expression for $g^{(2)}$ are given as follows:

$$\langle n_a \rangle_t = \bar{n} - \sum_{n=0}^{\infty} \tilde{P}_f(n)[1 - P_0(n, n, t)] ,$$

$$\langle n_b \rangle_t = \bar{n} + \sum_{n=0}^{\infty} \tilde{P}_f(n) P_2(n, n, t) , \qquad (6.5)$$

$$\langle n_a n_b \rangle_t = \bar{n}(2\bar{n} + 1) - \sum_{n=0}^{\infty} \tilde{P}_f(n)[n P_1(n, n, t) + P_2(n, n, t)] ,$$

while for the uncorrelated two-mode thermal and coherent states, we obtain

$$\langle n_a \rangle_t = \bar{n}_a - \sum_{n_a=0}^{\infty} \sum_{n_b=0}^{\infty} \tilde{P}_f(n_a, n_b)[1 - P_0(n_a, n_b, t)] ,$$

$$\langle n_b \rangle_t = \bar{n}_b - \sum_{n_a=0}^{\infty} \sum_{n_b=0}^{\infty} \tilde{P}_f(n_a, n_b) P_2(n_a, n_b, t) , \qquad (6.6)$$

$$\langle n_a n_b \rangle_t = \bar{n}_a \bar{n}_b$$
$$- \sum_{n_a=0}^{\infty} \sum_{n_b=0}^{\infty} \tilde{P}_f(n_a, n_b)[n_b P_1(n_a, n_b, t)$$
$$- (n_a - n_b - 1)$$
$$\times P_2(n_a, n_b, t)] .$$

From Eqs. (6.5) and (6.6) we see that the intensity of mode a is enhanced by the atom-field interaction, while that in mode b is diminished. This is of course due to the particular initial condition of the atom. Had we started in the excited level of the atom, we would have observed an increase in the intensity of both modes due to the spontaneous emission of an additional photon into the field.

In Fig. 9 we display the time evolution of the cross-correlation function for various values of the one-photon detuning. At zero detuning, we observe that the modes of the two-mode squeezed vacuum and the two-mode thermal state are correlated for all times, while those of the two-mode coherent state show both correlation and anticorrelation depending on the time of observation. As the detuning is increased, the modes of the two-mode squeezed vacuum and the two-mode thermal state remain correlated on the whole, but those of the two-mode coherent state are predominantly anticorrelated. As the photon distributions for the two-mode squeezed vacuum and the two-mode thermal state are much broader than the corresponding distribution for the two-mode coherent state, it seems that the spread in the initial photon number of the field plays an important part in determining the developments of correlations or anticorrelations between the field modes. In particular, it seems that the more sub-Poissonian the photon distribution is, *the greater is*
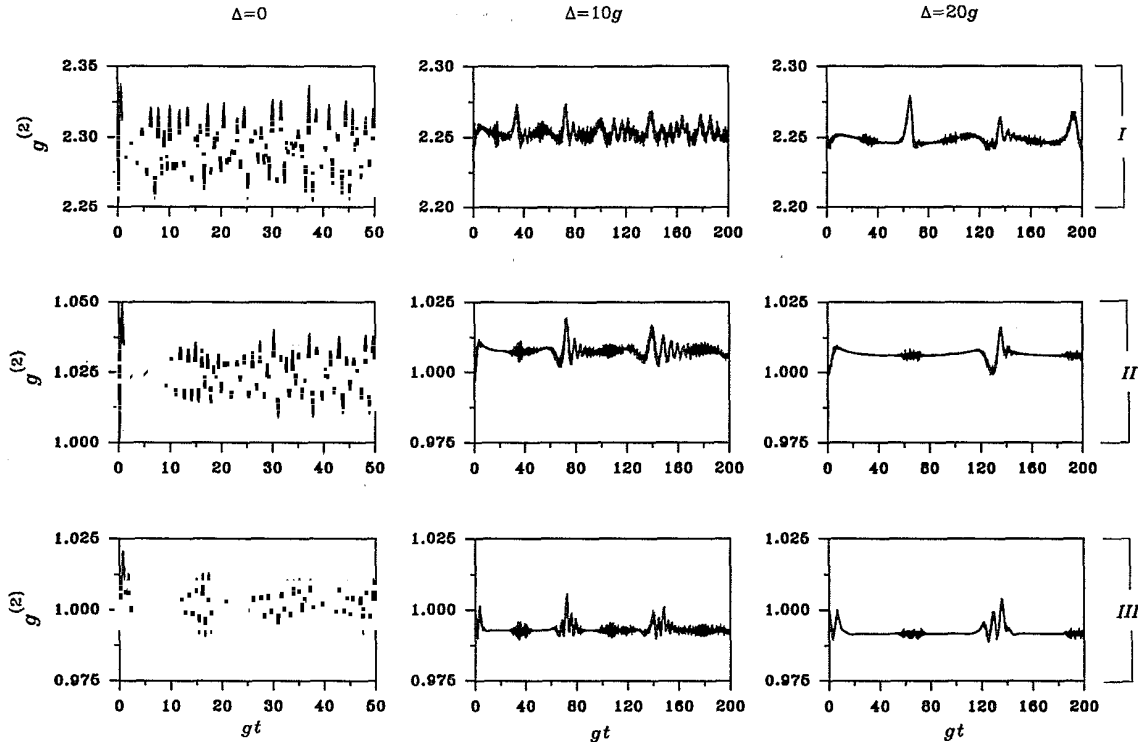
FIG. 9. Time evolution of the cross-correlation function for various initial states of the field. (*I*) two-mode squeezed vacuum, (*II*) two-mode thermal state, and (*III*) two-mode coherent state. The mean photon number in each mode is 4 and $g_a = g_b = g$.

the anticorrelation which will develop between the modes.

VII. TIME-AVERAGED FIELD DYNAMICS

The mean, time-averaged behavior of the field is determined by the time-averaged cross-correlation function

$$\bar{g}^{(2)} = \frac{\overline{\langle n_a n_n \rangle}}{\overline{\langle n_a \rangle \langle n_b \rangle}} \quad (7.1)$$

In Fig. 10 we plot $\bar{g}^{(2)}$ as a function of the one-photon detuning Δ. Whilst the modes of the two-mode squeezed vacuum and the two-mode thermal state remain correlated for all values of the detuning, curiously those of the two-mode coherent state are *anticorrelated* for sufficiently large values of the detuning. We observe further that the time-averaged correlation function saturates to a steady level for large detunings.

We can also study the time-averaged field dynamics by showing how $\bar{g}^{(2)}$ behaves as a function of the mean photon number in each mode. But rather than use $\bar{g}^{(2)}$, we will find it more convenient to use the quantity

$$\bar{C} = \frac{\bar{g}^{(2)} - g^{(2)}(0)}{g^{(2)}(0)} , \quad (7.2)$$

which is a measure of the deviation of the time-averaged cross-correlation function from the initial value of the cross-correlation $g^{(2)}(0)$. In Fig. 11 we display $\bar{C}$ as a

function of the mean photon number in each mode. Two values of the detuning were chosen, one at zero and the other at 20g, where $g = g_a = g_b$ is the atom-field coupling constant. At large mean photon numbers, the time-
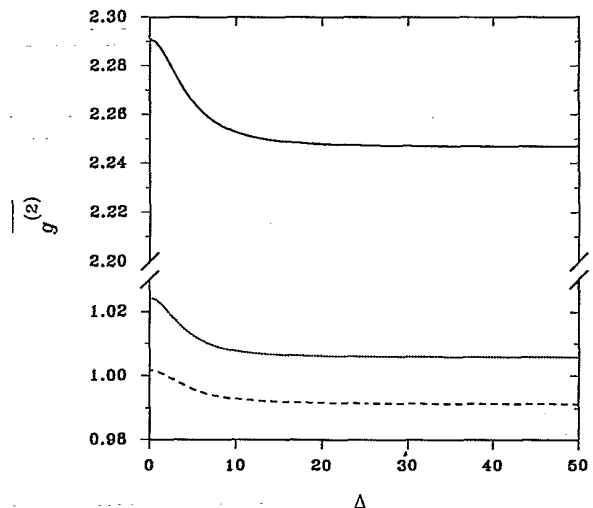

FIG. 10. Time-averaged cross-correlation function vs one-photon detuning. The solid, dotted, and dashed lines are for the two-mode squeezed vacuum, the two-mode thermal state, and the two-mode coherent state, respectively. The mean photon number in each mode is 4 and $g_a = g_b = g$.
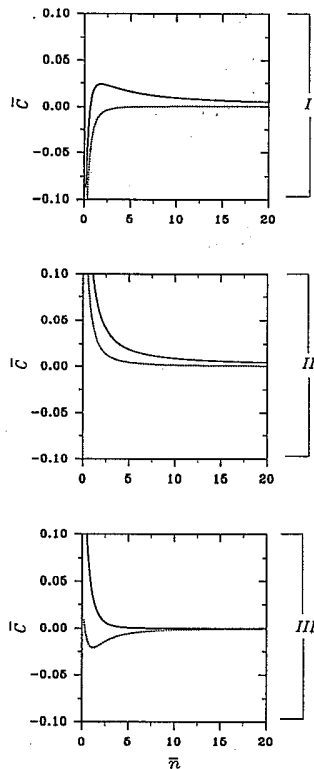
FIG. 11. Time-averaged deviation from the initial value of the cross-correlation function vs mean photon number in each mode. (*I*) two-mode squeezed vacuum, (*II*) two-mode thermal state, and (*III*) two-mode coherent state. The solid and dotted lines are for $\Delta=0$ and $\Delta=20g$, respectively. The atom-field coupling constants in all cases are $g_a=g=1$.

averaged field dynamics are hardly changed by the atom-field interaction. Further, for the two-mode coherent state, there is an optimum value for the anticorrelation between the modes, and this is reached at a moderate

mean photon number. Finally, we note that at small mean photon numbers, we could clearly distinguish between correlated and uncorrelated states of the field through a measurement of $\bar{C}$.

VIII. CONCLUSION

We have studied in detail the dynamics of a three-level atom in the λ configuration interacting with correlated and uncorrelated states of the electromagnetic radiation field. We showed that when the individual modes of the field are detuned by large amounts from the intermediate atomic level, the Rabi oscillations of the system dynamics are periodic and revive independently of the intensity of the initial field. We have attributed this to the linear dependence of the effective Rabi frequency on the photon numbers of the field modes. We found in particular that the revival times of the Rabi oscillations for the two-mode squeezed vacuum are in general smaller than those for the uncorrelated two-mode states, and that this is entirely due to the initial correlation which exists between the modes. We have demonstrated the role of Stark shifts in the system dynamics of the Raman coupled model studied by Gerry and Eberly [19] and by Knight [20], and showed that they cannot in general be neglected. Finally, we studied the influence of the atom-field interaction on the field dynamics. We showed that the photon distributions are greatly altered from their initial forms by the atom-field interaction. We examined the anticorrelation between the field modes and found that, whereas the modes of the two-mode squeezed vacuum and the two-mode thermal state are correlated by the atom-field interaction, those of the two-mode coherent state are anticorrelated by the atom-field interaction.

*Permanent address: Institute of Physics, Slovak Academy of Sciences, Dúbravská cesta 9, 842 28 Bratislava, Czechoslovakia.

[1] See, e.g., P. Meystre and M. Sargent, *Elements of Quantum Optics* (Springer-Verlag, Berlin, 1990).

[2] E. T. Jaynes and F. W. Cummings, Proc. IEEE **51**, 89 (1963).

[3] J. H. Eberly, J. J. Sanchez-Mondragon, and N. B. Narozhny, Phys. Rev. Lett. **44**, 1323 (1980); N. B. Narozhny, J. J. Sanchez-Mondragon, and J. H. Eberly, Phys. Rev. A **23**, 236 (1981); H.-I. Yoo, J. J. Sanchez-Mondragon, and J. H. Eberly, J. Phys. A **14**, 1383 (1981).

[4] P. Meystre and M. S. Zubairy, Phys. Lett. **89A**, 390 (1982); J. R. Kuklinski and J. Madajczyk, Phys. Rev. A **37**, 3175 (1988); P. K. Aravind and Guanghui Hu, Physica C **150**, 427 (1988).

[5] G. Rempe and H. Walther, Phys. Rev. A **42**, 1650 (1990).

[6] D. Meschede, H. Walther, and G. Müller, Phys. Rev. Lett. **54**, 351 (1985); G. Rempe, H. Walther, and N. Klein, *ibid.*

58, 353 (1987); G. Rempe, F. Schmidt-Kaler, and H. Walther, *ibid.* **64**, 2783 (1990). Squeezing at microwave frequencies has recently been demonstrated by Yurke *et al.* [B. Yurke, P. G. Kaminsky, R. E. Miller, E. A. Whittaker, A. D. Smith, A. H. Silver, and R. W. Simon, Phys. Rev. Lett. **60**, 764 (1988)] using a Josephson-parametric amplifier.

[7] B. Buck and C. V. Sukumar, Phys. Lett. **81A**, 132 (1981); C. V. Sukumar and B. Buck, *ibid.* **83A**, 211 (1981); J. Phys. A **17**, 885 (1984).

[8] H.-I. Yoo and J. H. Eberly, Phys. Rep. **118**, 234 (1985), and references therein.

[9] M. Tavis and F. W. Cummings, Phys. Rev. **170**, 379 (1968); F. W. Cummings and A. Dori, Phys. Lett. **95A**, 263 (1983).

[10] W. K. Lai, V. Bužek, and P. L. Knight, Phys. Rev. A **44**, 2003 (1991).

[11] V. Bužek and Tran Quang, J. Opt. Soc. Am. B **6**, 2447 (1989).

[12] See, e.g., the review by R. Loudon and P. L. Knight, J. Mod. Opt. **34**, 709 (1987).

[13] S. M. Barnett and P. L. Knight, J. Opt. Soc. Am. B **3**, 467 (1985); J. Mod. Opt. **43**, 841 (1987).

[14] P. M. Radmore and P. L. Knight, Phys. Lett. **90A**, 342 (1982).

[15] M. Takatsuji, Phys. Rev. A **11**, 619 (1975); P. W. Milonni and J. H. Eberly, J. Chem. Phys. **68**, 1602 (1978). Recently, Nayak and Bartiz [N. Nayak and V. Bartiz, Phys. Rev. A **42**, 2953 (1990)] studied the differences in the dynamics of a three-level and a two-level Rydberg atom interacting with two nondegenerate cavity modes, the two-level system being described by an effective Hamiltonian; see also A. W. Boone and S. Swain, Opt. Commun. **73**, 47 (1989).

[16] X.-S. Li and N.-Y. Bei, Phys. Lett. **101A**, 169 (1984).

[17] N. N. Bogolubov, Jr., F. L. Kien, and A. S. Shumovsky, Phys. Lett. **107A**, 456 (1985).

[18] X.-S. Li and Y.-N. Peng, Phys. Rev. A **32**, 1501 (1985).

[19] C. C. Gerry and J. H. Eberly, Phys. Rev. A **42**, 6805 (1990).

[20] P. L. Knight, Phys. Scr. **T12**, 51 (1986); see also S. J. D. Phoenix and P. L. Knight, J. Opt. Soc. Am. B **7**, 116 (1990).

[21] H. M. Moya-Cessa, V. Bužek, and P. L. Knight, Opt. Commun (to be published).

[22] R. E. Slusher, L. W. Hollberg, B. Yurke, J. C. Mertz, and J. F. Valley, Phys. Rev. Lett. **55**, 2409 (1985).

[23] S. M. Barnett and S. J. D. Phoenix, Phys. Rev. A **40**, 2404 (1989).

[24] See, e.g., R. Loudon, *The Quantum Theory of Light* (Oxford University Press, Oxford, 1973).

[25] J. D. Cresser and M. Hillery, Phys. Rev. A **40**, 1464 (1989); M. Hillery and R. J. Schwartz, *ibid.* **43**, 1506 (1991).